PROCEEDINGS OF SCIENCE

Simulation of radiopulses from Atmosphere-Skimming Extensive Air Showers with ZHAireS-RASPASS.

Matias Tueros[a,*]

[a] *Instituto de Fisica La Plata, CONICET-UNLP, Diagonal 113 entre 63 y 64 , La Plata, Argentina*

E-mail: tueros@fisica.unlp.edu.ar

Earth-skimming neutrinos and Atmosphere-skimming neutrinos or cosmic rays can induce extensive air showers that present some peculiarities in comparison to the better-characterized down-going showers. For some geometries, cascades can take place high in the atmosphere and develop over several hundred of kilometers, giving ample time for the geomagnetic field to deflect the particles. For other geometries, cascades can develop very close to the ground where the density is high and the resulting cascades are very short. Development in a thinner or denser atmosphere will shift the balance between the average interaction length and decay length of particles, giving showers that can have very different hadronic/electromagnetic components with respect to regular down-going showers. In this article we will showcase ZHAireS-RASPASS, a custom-built modification to the ZHAireS suite capable of simulating Atmosphere-Skimming and up-going (from Earth-skimming) showers and their radio-emission, focusing on how it could be used to inform the design and data interpretation of balloon-borne and satellite-borne experiments.

9th International Workshop on Acoustic and Radio EeV Neutrino Detection Activities - ARENA2022
7-10 June 2022
Santiago de Compostela, Spain

*Speaker

https://pos.sissa.it/

PoS(ARENA2022)056

1. Introduction

Atmosphere-Skimming showers are particle cascades initiated in the atmosphere by primaries whose incoming trajectory don't intersect the earth's surface. Balloon-borne experiments like ANITA [1], PUEO [2] and EUSO-SPB [3], satellite-borne experiments like POEMMA [4] and even ground based detectors like the Pierre Auger Observatory HEAT fluorescence detectors [5] are or could be capable of detecting these type of events.

The main characteristics of Atmosphere-skimming (AS) cascades are determined primarily by two parameters: the minimum distance between the shower trajectory and the earth's surface (the shower "impact parameter") and the the orientation of the magnetic field with respect to the shower direction of motion. An impact parameter of 0Km corresponds to regular horizontal showers, that are already quite different from the regular down-going (DG) ones. But more extreme differences arise when the impact parameter is several kilometers. In this case the shower starts developing from a zone of low density into a zone of higher density, as a regular DG shower, but will emerge again into a decreasing density zone. This results in a particle cascade that develops over several hundred of kilometers, that can even escape the atmosphere, and that has ample time for the local magnetic field B to deflect the particles and create a significant net charge separation. Several effects can rise from this separation, depending on the orientation of the magnetic field with respect to the shower direction of motion. For example in the south pole where the magnetic field is almost perpendicular to the earth surface the shower creates a horizontal fan of particles, making the shower very wide in the plane parallel to the surface (optimal to be seen from above). On the equator, were the magnetic field is parallel to the surface, the shower fans in the plane perpendicular to the surface. Particles plunging deeper into the atmosphere are attenuated faster than particles deflected upwards, creating a distinct asymmetry. In both cases, low energy particles can be trapped in the magnetic field lines and kept gyrating up in the rarefied atmosphere.

Little progress has been done on understanding the influence that these effects can have on the detection of AS cascades through their radio, fluorescence or Cherenkov signatures. Some analytical calculations and the proposal of several novel detection techniques where carried by D. Fargion and collaborators [6], but detailed Monte Carlo simulations of these type of events where still missing, due to the lack of microscopic shower simulation tools capable of handling these geometries. Enter ZHAireS-RASPASS.

2. ZHAireS-RASPASS

RASPASS is an **A**ires **S**pecial **P**rimary for **A**tmospheric **S**kimming **S**howers. Born in 2011 as an Aires [7] special primary module to study ANITA direct events, it evolved into a stand alone version of ZHAireS [8] (Called ZHAireS-RASPASS), that includes several modifications to allow for the simulation of up-going, down-going, earth-skimming and atmosphere-skimming showers. It features the same physics algorithms from the standard ZHAireS (and the same limitations), the same user-friendly input of Aires, and it adds the capability to simulate showers initiated by multiple primaries (as for example the decay products of tau decay) in any event geometry.

In ZHAireS/Aires, geometry is controlled by the shower zenith and azimuth angles, defined with respect to a vertical axis located at the shower core position. Since core position has no

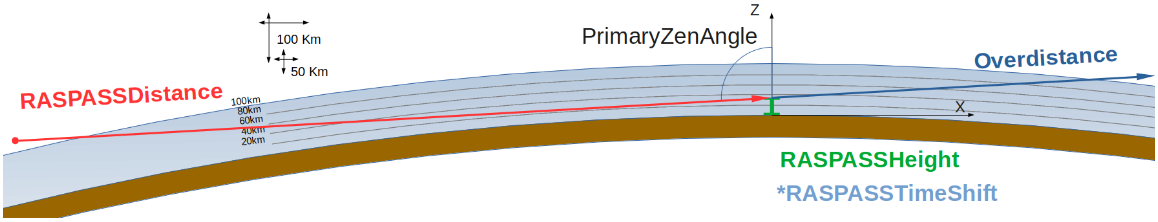

Figure 1: Geometry of an Atmosphere-Skimming event with impact parameter 24,7Km., corresponding to a 93.25 deg zenith shower passing at 35km altitude (RASPASSHeight), injected 1500km from the Z axis (RASPASSDistance) and tracked an additional 725km (Overdistance), showing the earth curvature to scale.

meaning in earth skimming showers, in RASPASS (see Fig 1) the geometry is controlled by two additional directives, *RASPASSHeight*, which controls the height at which the shower axis intersects the vertical axis and *RASPASSDistance*, which specifies the distance from the injection point to the vertical axis. An optional directive, *RASPASSTimeShift*, can be used to control the injection time if needed, and a compilation parameter *Overdistance* controls how far beyond the vertical axis the longitudinal development of the cascade is tracked.

The more important limitations of Aires/ZHAireS inherited by RASPASS are the use of a single-layer exponential model for the index of refraction and the use of a constant magnetic field (which does not follow the earth curvature). These limitations are easy to overcome at the expense of CPU time. For now, these approximations are good enough to study the general characteristics of AS showers.

3. Example of Aplicattion to Baloon-borne Experiments

To showcase the capabilities of ZHAireS-RASPASS, and the rich phenomenological palette presented by AS showers, we start by looking at what an AS cascade looks like when propagating on a magnetic field that is mainly pointing down, like in the south pole. In Fig. 2 we show the trajectories of the particles of a cascade produced by a 100 TeV Proton coming from the left. Using Fig. 1 to guide our discussion (this shower has a slightly higher impact parameter of 32Km), we see that the primary is injected very high in the atmosphere, where density is extremely low. The cascade only begins once the air density starts to increase, as the particle plunges deeper in the atmosphere. The point of minimum height and maximum density is 224Km to the left of the center of the figure. Muons, positrons and electrons produced at the beginning of the cascade loose their energy fast, as they move towards a denser media. Tracks are shorter and many small circumferences from low energy electrons and positrons can be seen. Particles appearing farther away from the shower axis are produced by the cascade gammas, not shown. A lone low energy neutron, originated on a nuclear collision, escapes the cascade without deflection. As the cascade approaches the center, it is propagating towards higher altitudes and a thinner atmosphere. Particles loose less energy and have fewer interactions, and can keep propagating around the field lines. Some of them follow the field lines upwards, into a even thinner atmosphere increasing their free path, while others follow them downwards and are stopped faster. High energy electrons and muons end escaping the atmosphere.

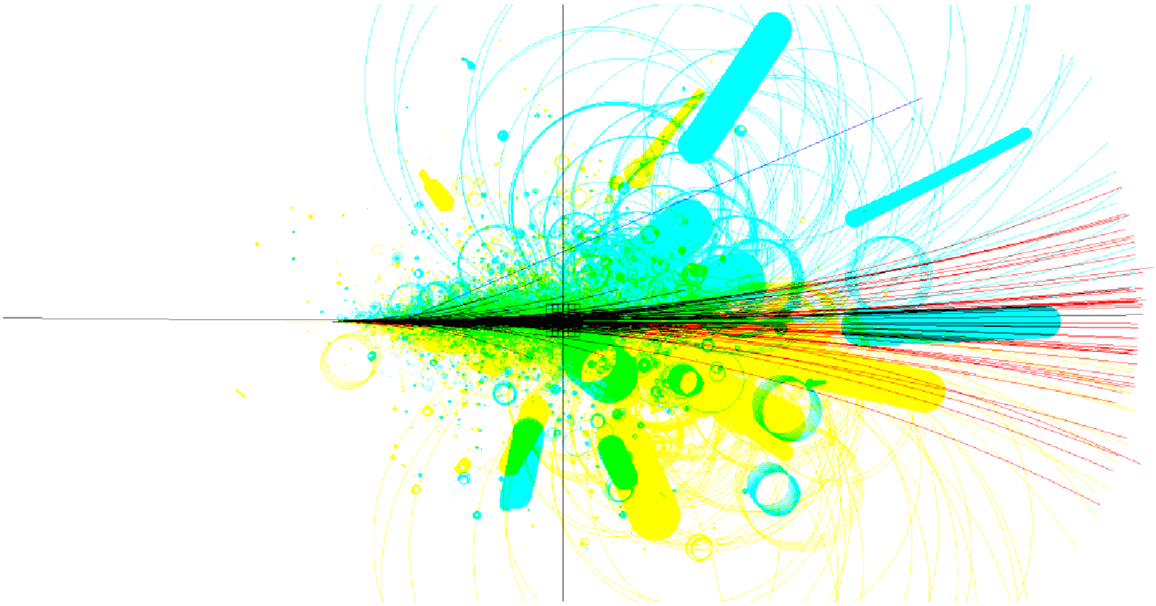

Figure 2: Top view of a shower produced by a 100 TeV proton grazing the atmosphere incoming from the north (on the left side) at 32Km impact parameter. The shower develops over nearly 2000km. The small grid displayed in the center has elements of 10km by 10km for scale. Muons (red), electrons (yellow), positrons (cyan) and neutrons (blue) give additional colors when tracks are superimposed.

3.1 Shower Longitudinal profiles

The interplay of density and shower propagation can be studied in more detail by looking at cascades using different impact parameters, and thus changing the total traversed mass and the maximum atmospheric density experienced by the cascade. This is equivalent to changing RASPASSHeight in the geometry of Fig. 1.

Figure 3 shows the number of e^+/e^- as a function of both the total traversed mass since injection and the distance from the z axis, where a balloon-borne detector could be located, for primary protons of 10 EeV injected 1500Km away with a 93.25 Zenith angle (3.5 degrees below the horizontal). In this example, protons travel more than 500Km without interacting (density is so low, this is less than 100 g/cm^2). The atmospheric density profile that each shower experiences is different, but as long as there is enough mass, all longitudinal profiles look similar. For the highest impact parameter, 29.7Km at RASPASSHeight 40Km, there is not enough mass for the cascade to fully develop before reaching the detector. The lower total number of e^+/e^- is a consequence of a lower number of low energy particles, but the total energy content in the electromagnetic cascade is similar, as can be seen in Fig. 4.

Even if longitudinal profiles are similar, the place in the atmosphere where they occur is different. This is very important for radio detectors, as the index of refraction at each shower maximum will be different. Cascades with a lower impact parameter occur farther away from the detector and in a denser atmosphere, resulting in a wider Cherenkov cone at the detector. Showers with a high impact parameter occur closer to the detector, making them difficult to detect, if not outright impossible do to the loss of coherence in the radio emission, as we will see in the next section.

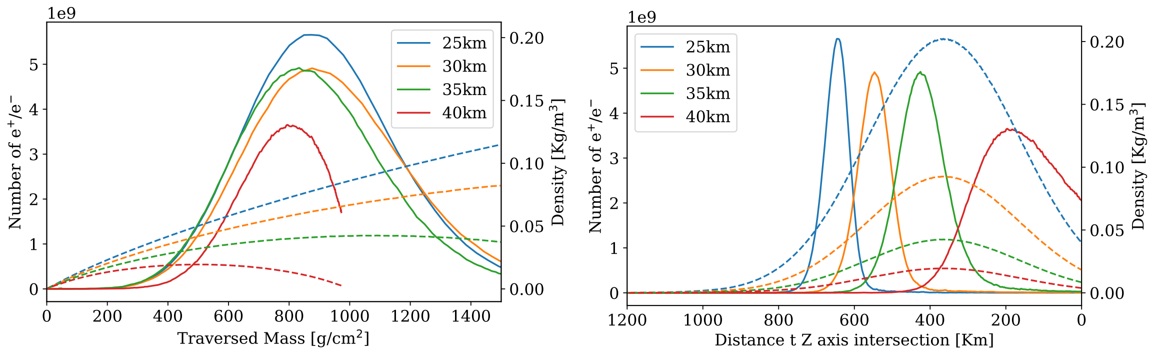

Figure 3: Total number of e$^+$/e$^-$ as a function of traversed mass (left) and distance along the shower axis (right) for different RASPASSHeight, corresponding to impact parameters of 14.7, 19.7, 24.7 and 29.7Km

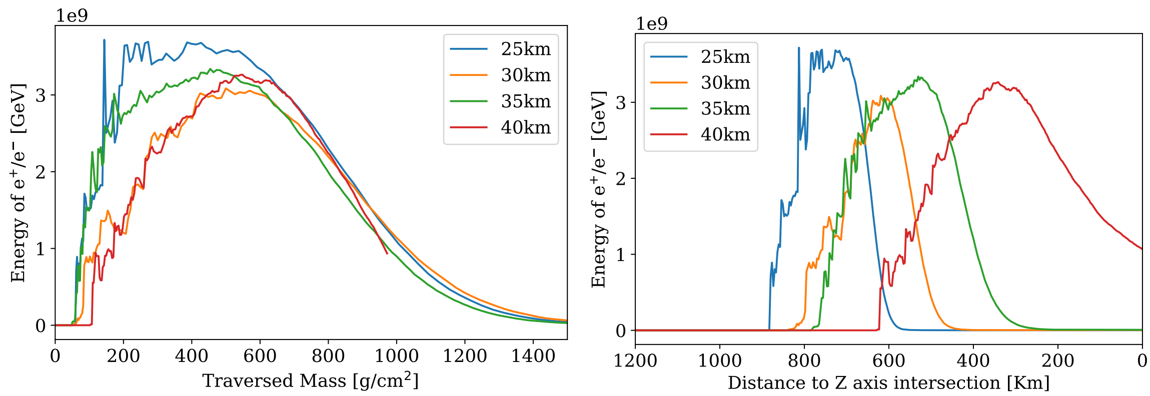

Figure 4: Total energy of e$^+$/e$^-$ as a function of traversed mass (left) and distance along the shower axis (right) for different RASPASSHeight, corresponding to impact parameters of 14.7, 19.7, 24.7 and 29.7Km

3.2 Signal Lateral Distribution

The signal amplitude for a set of detectors located along an horizontal line perpendicular to the shower trajectory (the Y axis in our reference frame), at the intersection with the Z axis of Fig. 1, is shown on the left panel of Fig. 5. In this example, a shower with RASPASSHeight 25km would be easier to detect despite being father away from the detector, spread over a wider ring. The 40km RASPASSHeight cascade ends up being so close to the detector (the detector would actually be *inside* the cascade) that it can not be detected. Another peculiarity of AS cascades is made evident when investigating the signal on detectors along the Z axis, shown in the right panel of Fig. 5. Since the atmospheric profile above and below the shower axis differ significantly, the optical paths are different and the Cherenkov cone is not symmetric. This effect is akin to the refractive displacement of the Cherenkov cone described in [9].

3.3 Coherence Asymmetry

The shower fanning due to the magnetic field introduces a new additional asymmetry, that we will call the Coherence Asymmetry. The characteristic shower dimensions are different for observers above/below the shower than for observers left/right of the shower. Observers seeing the

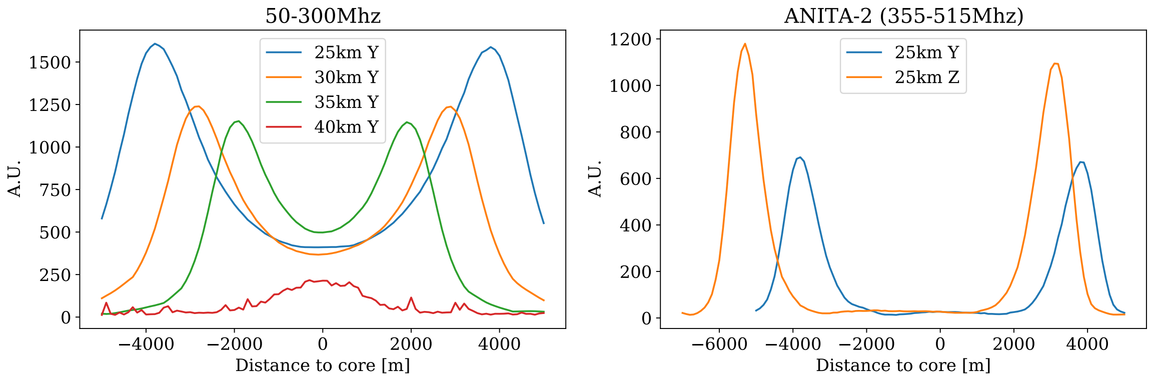

Figure 5: Signal amplitude in the 50-300Mhz range as a function of the lateral distance on a horizontal axis (left) and in the 355 to 515MHz - One of ANITA trigger windows - along the vertical Z axis (right) for different values of RASPASSHeight, for a 93.25 deg zenith incoming direction.

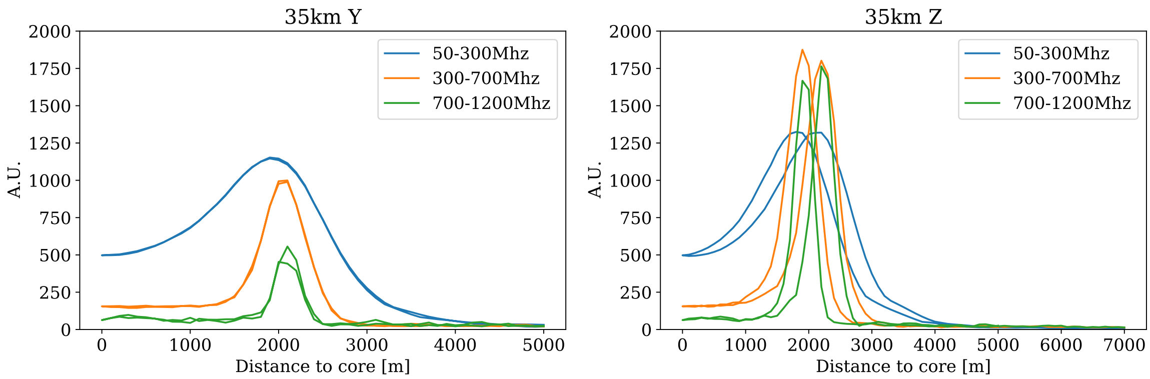

Figure 6: Signal amplitude in different frequency windows as a function of the lateral distance along the horizontal (left) and vertical (right) axis for 35Km RASPASSHeight, 93.25 incoming zenith direction.

shower from the side, where the shower is extended and see the signal arrive more dispersed in time, with a lower high frequency content. Observers above/below the shower fan see the emission from the shower arriving more coherently and thus with a higher frequency content. This effect, accompanied by the refractive effect mentioned in the previous section, is illustrated in Fig. 6, where the signal amplitude at both sides (left) and on top and bottom of the shower (right) are displayed in different frequency bands. This effect can be important when using different frequency windows for triggering. On the other hand, the relative difference between the signal in different frequency windows carries information on the relative position of the shower and the detector, and could be exploited to reconstruct the event axis. This effect is also present on very inclined DG cascades, but has not been detected until now because the effect can be seen only at frequencies above current and proposed surface experiments, like the Auger Radio upgrade [10] or GRAND [11].

3.4 Geometry Phase-Space

The dependence of the width of the Cherenkov cone with altitude, and its above-mentioned asymmetries, make the calculation of the effective area of balloon-borne experiments altitude

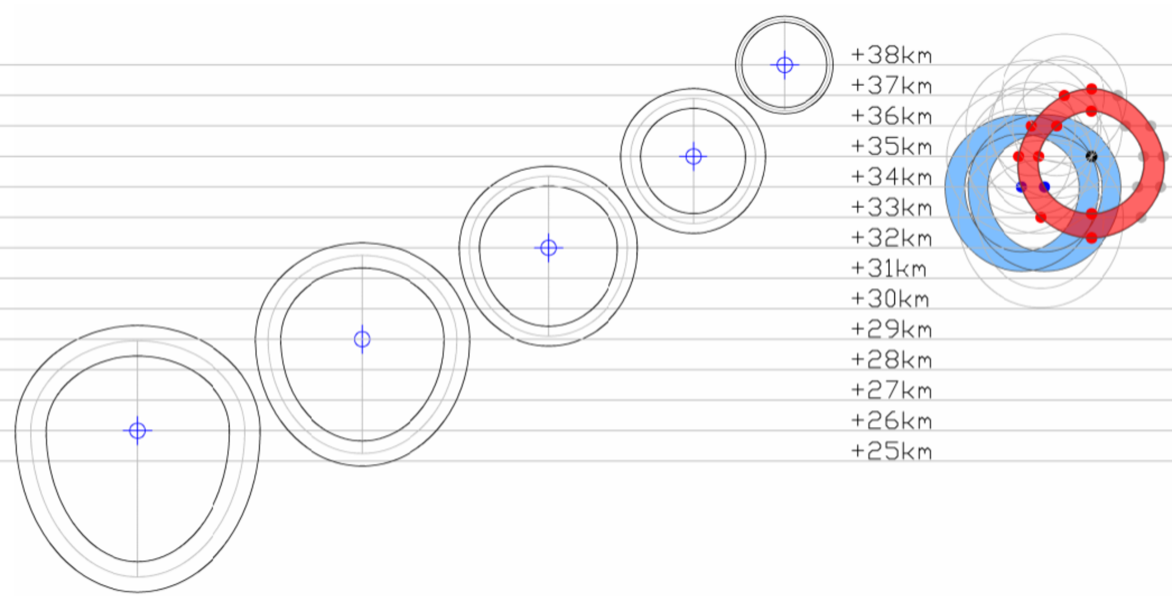

Figure 7: Trigger area around a Atmosphere-Skimming cascade incoming at 93.25 deg, for different RASPASSHeight values. For a Balloon-borne experiment hovering at 35 Km, the composition of all the trigger areas give the effective trigger area, shown in red on the right.

dependent, and difficult to estimate. For each shower incoming direction the "triggerable area" of the shower changes with the shower altitude, as shown on the left side of Fig. 7. A detector hovering at a fixed altitude can only see showers passing at a certain distance from it, such that the detector falls inside the shower triggerable area. Since the triggerable area depends on the shower altitude, the detector effective area is not a ring, but a somewhat irregular shape. This shape changes with the incoming shower direction. In order to evaluate the detector total effective area, the phase-space of incoming directions and shower altitudes needs to be covered. This phase-space varies slightly for each detector altitude . Figure 8 shows an example of the phase-space that needs to be covered for a detector at 35Km altitude. Note that from the 4 showers presented in the previous figures, only the 35Km one has a chance of being detected (if it where to pass between 1 and 3km to the side of the detector). The shower at 30 Km would never be detected, as its Cherenkov cone is only between 2 and 3.5 km in radius. The shower at 40km has not enough mass to develop before reaching the detector and even worse, is too high to be detected.

4. Conclusions

We have shown some of the characteristics of Atmosphere-Skimming cascades, and showcased some counter-intuitive effects like showers farther away being easier to detect than showers closer to the detector or the coherence asymmetry between observers above/below the shower and observers to the side of the cascade. Atmosphere-Skimming cascades can open new detection channels for old techniques or justify the development of new techniques, but complex and detailed simulations are required to accurately asses their relevance and feasibility. This is now possible to investigate using ZHAireS-RASPASS, which is available upon request to the author.

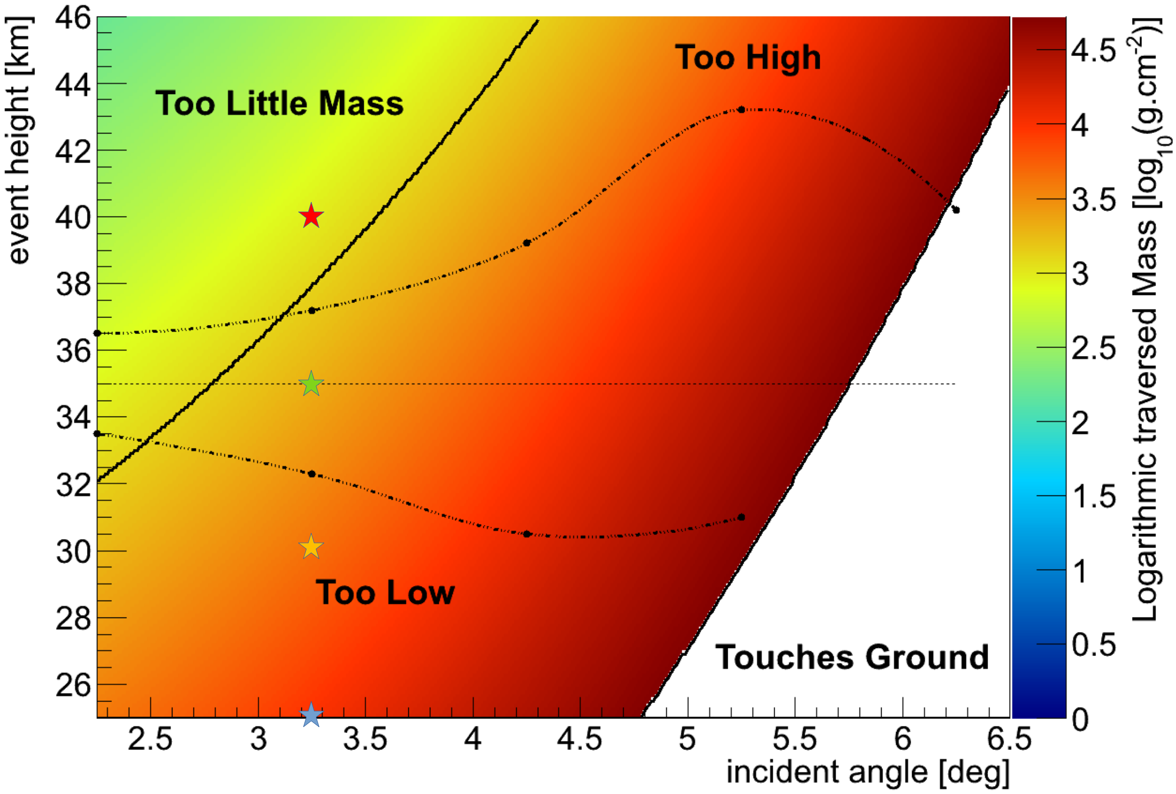

Figure 8: Phase space that needs to be explored for trigger studies of a balloon-borne radio experiment hovering at 35Km height. Stars show the geometry of the vents shown in Figs. 3 and 4. The area inside the dashed lines and to the right of the solid line is where there is some possibility for the events to be detected.

References

[1] R Pretchet et al. Phys. Rev. D 105, 042001 [arXiv:2112.07069] and references therein

[2] Q. Abarr et al. JINST 16 (2021) 08, P08035, [arXiv:2010.02892]

[3] J. Eser et al., PoS ICRC2021 (2021) 404

[4] A.V. Olinto et al., JCAP 06 (2021) 007,[arXiv:2012.07945]

[5] C. Meurer et al. Astrophys. Space Sci. Trans., 7, 183-186, 2011 [arXiv:1106.1329]

[6] D. Fargion et al. PoS ICRC2021 (2021) 1208 and references therein

[7] S. J. Sciutto, [arXiv:astro-ph/9911331]; http://aires.fisica.unlp.edu.ar.

[8] J. Alvarez-Muñiz et al., Phys.Rev.D 86 (2012) 123007,[arXiv:1208.0951]

[9] F. Schlüter et al., Eur. Phys. J. C 80, 643 (2020) [arXiv:2005.06775]

[10] Pierre Auger Collaboration, Science Reviews - from the end of the world (Argentina) Vol. 1, No. 4 (2020) 8-33.

[11] J. Alvarez-Muñiz et al., Sci. China-Phys. Mech. Astron. 63, 219501 (2020) [arXiv:1810.09994]